Max-Planck-Institut
für Quantenoptik
BIBLIOTHEK
D-8046 Garching

THE EVOLUTION OF TWO-DIMENSIONAL EFFECTS IN FAST ELECTRON TRANSPORT FROM HIGH INTENSITY LASER PLASMA INTERACTIONS

MPQ 60 April 1982

MPQ

MAX-PLANCK-INSTITUT FÜR QUANTENOPTIK

8046 GARCHING BEI MÜNCHEN

MPQ-Report
60

MAX-PLANCK-INSTITUT FÜR QUANTENOPTIK

THE EVOLUTION OF TWO-DIMENSIONAL EFFECTS IN FAST ELECTRON TRANSPORT FROM HIGH INTENSITY LASER PLASMA INTERACTIONS

MPQ 60 April 1982

F. Amiranoff[a], K. Eidmann, R. Sigel,
R. Fedosejevs[b], A. Maaswinkel,
Yung-lu Teng[c]

Max-Planck-Institut für Quantenoptik
D-8046 Garching, Federal Republic of Germany

J.D. Kilkenny, J.D. Hares, D.K. Bradley,
B.J. MacGowan, T.J. Goldsack

The Blacket Laboratory
Imperial College of Science and Technology
London SW7 2BZ, U.K.

Max-Planck-Institut
für Quantenoptik
BIBLIOTHEK
D-8046 Garching

(a) Present address: Ecole Polytechnique, F-91128 Palaiseau, Cedex, France.
(b) Present address: Department of Electrical Engineering, The University of Alberta, Edmonton, Alberta, Canada, T6G 2G7.
(c) Present address: Shanghai Institute of Optics and Fine Mechanics, Academia Sinica, Shanghai, People's Republic of China.

This work was supported by the Bundesministerium
für Forschung und Technologie and Euratom.

MPQ 60

THE EVOLUTION OF TWO-DIMENSIONAL EFFECTS IN FAST ELECTRON TRANSPORT FROM HIGH INTENSITY LASER PLASMA INTERACTIONS

Abstract

Measurements of local and remote energy deposition by fast electrons have been made in 1.3 μm and 1.05 μm laser irradiation experiments with plane targets and various pulse lengths. From optical and X-ray streak photography and spatially resolved Kα yield measurements it is found that up to 30% of the absorbed laser energy spreads laterally to distances of several millimeters from the focal spot with a spreading velocity in excess of 10^8 cm sec^{-1}.

SHORT TITLE: Radial energy transport from laser produced plasmas

INSPEC Classification Number: 5250J

When an intense laser beam is incident on a solid target a fraction of its energy is absorbed in the dense plasma cloud which is produced during the interaction. At the high irradiance of interest to laser fusion the subsequent transport of energy away from the absorption region is complicated by the coupling of a major fraction of the absorbed energy into very fast, so-called suprathermal electrons. These high energy electrons are nearly collisionless in the plasma cloud which expands at velocities up to several 10^8 cm sec^{-1}. After reflection at the plasma cloud boundary, instead of entering the solid target under the small focal spot, they may deposit their energy many millimetres away, leading to a very high rate of lateral spreading of energy. The trajectories may be further complicated by intense electric and magnetic fields existing in the plasma. Investigation of such effects is of interest for laser fusion as they affect the uniformity of energy deposition in laser fusion targets. Furthermore they complicate the interpretation of model experiments, in particular those using planar targets, which might become two dimensional in nature in the presence of strong lateral spreading.

Recently sideways spreading of energy has been observed, albeit semi-qualitatively, for 10.6μm irradiation (Ebrahim 1979, Jaanimagi 1981, Decoste 1981). Ebrahim (1979) has measured the ion emission from the front and rear sides of

disc targets irradiated with 10.6μm laser pulses and has inferred large energy transport to the rear surface. In this paper we present the first quantitative experiments in which the amount and rate of sideways energy spreading in 1.05μm and 1.3μm irradiation experiments are measured. We show that the radially spread energy, or remote deposition, which enters the target can exceed the energy deposition beneath the focal spot. The results were obtained in a collaboration between British and German groups using the Rutherford Laboratory Central Laser Facility (λ = 1.05μm) and the Asterix III iodine laser (λ = 1.3μm) at Garching.

The two laser facilities enabled single beam experiments to be performed over a wide range of illumination conditions as listed in Table I. Planar targets of various shapes and materials were used in all experiments at near normal incidence ($\leq 10^0$). The diagnostics used were high speed photography with a synchronised 10psec dye laser pulse, multiple X-ray pinhole camera arrays filtered for target Kα emission, an X-ray streak camera for time and space resolution of the Kα emission and a time integrating crystal spectrometer to measure the Kα emission from the focal area (Hares 1979).

Two-dimensional, time-resolved information (though qualitative with respect to energy deposition) on lateral spreading of energy is obtained from high-speed photography.

Fig. 1 shows a shadowgram, taken 2.2nsec after the 300psec laser pulse, of a 2μm thick plastic foil ribbon (~ 0.5mm wide) irradiated from the left. It is seen to explode over the whole field of view (~ 3mm in diameter). The relatively small size of the focal region is indicated by the bright spot in the centre of the photograph produced by the second harmonic of the laser light generated in the plasma. The time delay before the foil starts to explode was determined in a separate experiment using a streak camera whose slit was displaced laterally a distance δ as shown in Fig. 1. In this case the dye laser was operated in a long pulse mode. The streak photographs showed a sudden onset of foil expansion corresponding to a spreading velocity of 3.5×10^8 cm sec^{-1} for δ = 2mm. Quantitative measurements of the fast electron energy deposition were made using X-ray pinhole cameras and calibrated film. Images of the X-ray emission from these experiments taken with large (> 200μm diameter) pinholes are shown in Fig. 2. In each case there is a shadow of the pinhole formed by emission from the intense focal spot and a spatially resolved image of emission remote (> 200μm) from the focal spot. Pairs of pinholes were used with the filtering chosen such that the difference between the two images was due to emission in the region of the Kα line of the target material.

In Fig. 2a, for which a 1mm wide vanadium strip was

irradiated at $5 \pm 2 \times 10^{15}$ W cm^{-2}, there is a clear difference in the images of the spread emission through these two filters. The filters were chosen such that V Kα emission produces a large difference in the brightness of the recorded images whereas a continuum of the form $I_0 \exp(-h\nu/kT)$ only produces a small difference. This difference is a factor of 1.5 for a typical fast electron continuum tempeature of 10keV. Plasma line emission such as V XXII $1s^2$ - 1s2p is strongly attenuated by both filters. The spread emission in the top image is ~8 times brighter than the lower image and is attributable to V Kα emission. A continuum cannot produce such a large difference.

The Kα emission is due to electron K shell ionisation and not K shell photoionisation. In Fig. 2a this is clear from the assymetry; also spectra show that the main plasma emission from the central spot is the V XXII $1s^2$ - 1s2p transition which cannot cause K shell photoionisation. Thus Fig. 2a shows that for a 300psec pulse electrons are depositing energy some millimetrs away from the focal spot with enhanced deposition at the edge of the target.

For Fig. 2b - 2c the fainter images through the Kα attenuating filter (not included) showed that the spread emission was dominantly Kα, as in Fig. 2a. Fig 2b, from a shot on a V target approximately 1cm square, also shows remote deposition, for an 80psec pulse, with an assymmetric

structure. The assymmetry was not reproducible, however the deposition was always greater at the edge of the spreading region, forming an irregular ring around the focal spot. The ring structure is more clear in Fig. 2c for a 300psec pulse on a large area target. For longer pulses, as in Fig. 2d, remote deposition, albeit not in a clear ring was also seen. Enhanced remote deposition at the target edge is clearly seen in Fig. 2e, the target for which was a 1mm square of Cu supported on a thin fibre.

The spreading observed by the static pinhole camera shown in Fig. 2 was time resolved using an X-ray streak camera. A streak record of Kα emission viewed at 10^0 to the target surface is shown in Fig. 3 for a 1.3nsec pulse. There is bright emission from the region of the focal spot at the bottom of the picture and clear evidence of sideways spreading away from the focal spot at a rate of $2.3 \pm 0.2 \times 10^8$ cm sec^{-1}. Time resolution shows that the emission peaks at the edge of the region for a 1.3nsec pulse. Streak records of 80psec experiments show a consideably higher spreading rate of $2.0 \pm 0.5 \times 10^9$ cm sec^{-1}.

The time integrated measurements of Kα emission can be used to determine the total energy that fast electrons deposit into the target. Characteristic X-ray emission has the property that if E_o, the energy of the incident electron, is

significantly greater than the K ionisation threshold, E_{KI}, then the ratio of fast electron induced Kα emission to total energy deposited by fast electorns, $R(E_o)$, is amost constant (Hares 1979). For a spectrum of fast electron energies (e.g. $f(E) = f_o \exp[-E/kT_h]$) $\bar{R}(T_h)$ can be computed. If $T_h > E_{KI}$ then $\bar{R}$ is insensitive to the exact form of the distribution function.

Experiments with various thicknesses of plastic coating over the fluor layer showed that for 300psec iodine laser pulses at 5×10^{15} W cm^{-2} the remote deposition is modelled by a distribution as above with $kT_h = 13 \pm 2$ keV. This observation completely rules out photoionisation as being a significant source of the emission since the drop in Kα yield with increasing plastic thickness is not consistent with the rather small attenuation by plastic of the greater than E_{KI} photon energies required to cause K-shell photoionisation. The total remote Kα yield was obtained from the X-ray pinhole images by integrating the exposure around the central pinhole shadow.

An alternative method was to use an edge to image, rather than a pinhole, such that the integration was automatically carried out to a large distance from the focal spot. The two techniques agreed with respect to the total Kα yield.

Values of the fractional remote energy deposition as shown

in Table I are thus obtained. For the 80psec and 1.3nsec experiments $\bar{R}$ was calculated using a value of T_h appropriate to the laser irradiance (Forslund 1977).

The local deposition was measured by an X-ray crystal spectrometer. For the 80psec and 300psec experiments the layered fluor target technique (Hares 1979) was employed: for the 1.3nsec experiments there was a much lower local deposition so a single element target was used. The spectrum indicated a bright source of Kα emission with f.w.h.m. < 200μm. This was attributed to local deposition beneath the focal spot. The fractional local depositions are shown in Table I. The local energy deposition can be seen to drop with increasing pulse length.

In summary we have shown that lateral transport, which has previously been observed in 10.6μm experiments, is energetically significant with shorter wavelengths, $\lambda \simeq 1\mu m$. We find that up to 30% of the absorbed energy is deposited in an area several millimetres in diameter; a fraction, which for 300psec and 1.3nsec pulses, exceeds that which enters the target under the focal spot. This remote energy deposition is over a depth in the target consistent with a fast electron distribution with $T_h \sim 10$ keV. The total fast electron energy deposition is broadly constant at ~ 10% of the incident laser energy for all our experiments, however the balance between local and remote deposition

depends on pulse length and, to a lesser extent, irradiance with longer pulses favouring remote deposition. It should be kept in mind that the numbers determined here represent a lower limit for lateral fast electron spreading as radiationless channels of enegy dissipation (e.g. via fast ion generation) were not considered.

Estimates of space charge limitation show that the fast electron power flow (~ 10% of the incident laser power) must be through a neutralizing background plasma rather than through the vacuum. The rapid formation of such a plasma cloud is in fact indicated by the emission of fast ions with velocities up to 7×10^8 cm sec^{-1} as measured a $\lambda = 1.3\mu m$ in a preceding investigation (Tsakiris 1981).

There was irreproducible assymmetry in the remote depositon in all experiments, coupled with a tendency for deposition to be greater at the edge of the spreading region, leading to a ring-like structure. This could be explained by the presence of a large toroidal magnetic field channelling electrons to the edge of the plasma cloud.

The spreading observed with 80psec pulses is inconsistent with the expansion of the fast ion cloud since the implied spreading rate (2×10^9 cm sec^{-1}) is too great. It is probable that in the 80psec experiments a plasma layer is formed on the target surface by X-rays, a few very energetic

fast electrons, laser light in the periphery of the focal spot or surface breakdown due to intense electric fields (Fedosejevs 1981). The assymmetries and ring structure, further complicated by the enhaced deposition at the target edge (Fig. 2e) make a quantitative model for our observations impossible at this stage.

ACKNOWLEDGEMENT

The 1.05μm experiments were performed at the Science and Engineering Research Council Central Laser Facility. The Royal Society and the D.F.G. provided support for travel.

REFERENCES

Decoste, R., Kieffer, J.C., Pepin, H., Phys.Rev.Lett. 47, 35 (1981)

Ebrahim, N.A., Joshi, C., Villeneuve, D.M., Burnett, N.H., Richardson, M.C., Phys.Rev.Lett. 43, 1995 (1979)

Fedosejevs, R., Yung-lu Teng, Sigel, R., Eidmann, K., Petsch, R., J.Appl.Phys. 52, 4186 (1981)

Forslund, D.W., Kindel, J.M., Lee, K., Phys.Rev.Lett. 39, 284 (1977)

Hares, J.D., Kilkenny, J.D., Key, M.H., Lunney, J.G., Phys.Rev.Lett. 42, 1216 (1979)

Jaanimagi, P.A., Ebrahim, N.A.. Burnett, N.H., Joshi, C., Appl.Phys.Lett. 38, 734 (1981)

Tsakiris, G.D., Eidmann, K., Petsch, R., Sigel, R., Phys.Rev.Lett. 46, 1201 (1981)

TABLE I. SUMMARY OF THE RADIAL TRANSPORT MEASUREMENTS

Laser parameters:																							
Irradiance (10^{15} W cm^{-2})	18 ± 6				2.0 ± 0.5				2.6 ± 0.5				6.0 ± 2.0				1.5 ± 0.5			
Wavelength (μm)	1.05				1.05				1.05				1.3				1.3			
Pulse length (psec)	80				1300				80				300				300			
Fractional absorption	.3				.3				.3				0.4				0.4			
Local deposition	7 ± 1				< 0.3				7 ± 1				1 ± 0.2				1 ± 0.2			
E_L/E_{INC} (%)																				
Remote deposition	10 ± 2				5 ± 1				1 ± 0.5				6 ± 1				6 ± 1			
E_R/E_{INC} (%)																				
Spreading rates	20 ± 10				2.5 ± 1				20 ± 10				3.5 ± 1.5				-			
(10^8 cm sec^{-1})																				

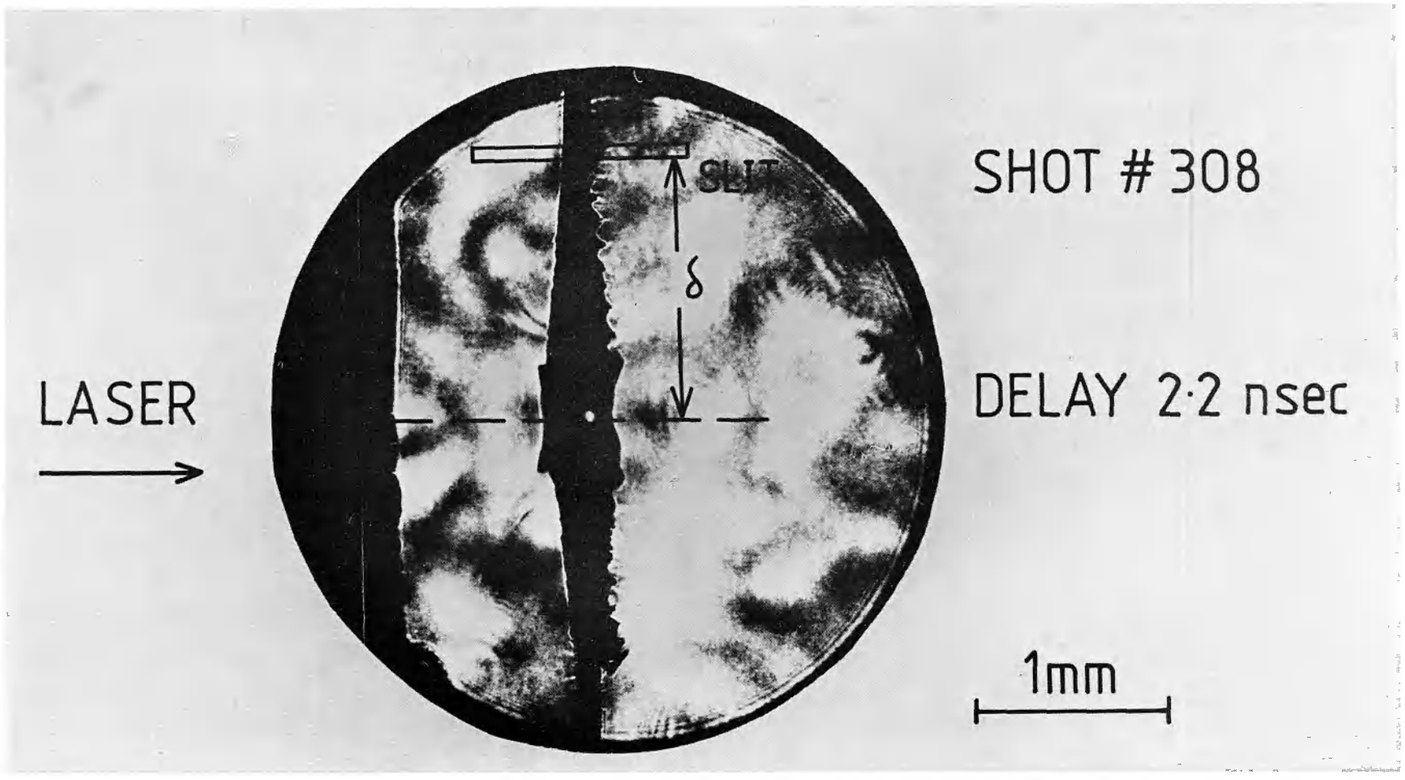

Fig. 1: Optical shadowgram showing a 2 μm thick, 500 μm wide plastic foil strip 2.2 nsec after irradiation from the left by a 1.3 μm laser pulse at an irradiance of 6×10^{15} W cm^{-2}. The rate of lateral energy spreading was obtained from streak photographs with the slit displaced a distance δ from the focus as shown.

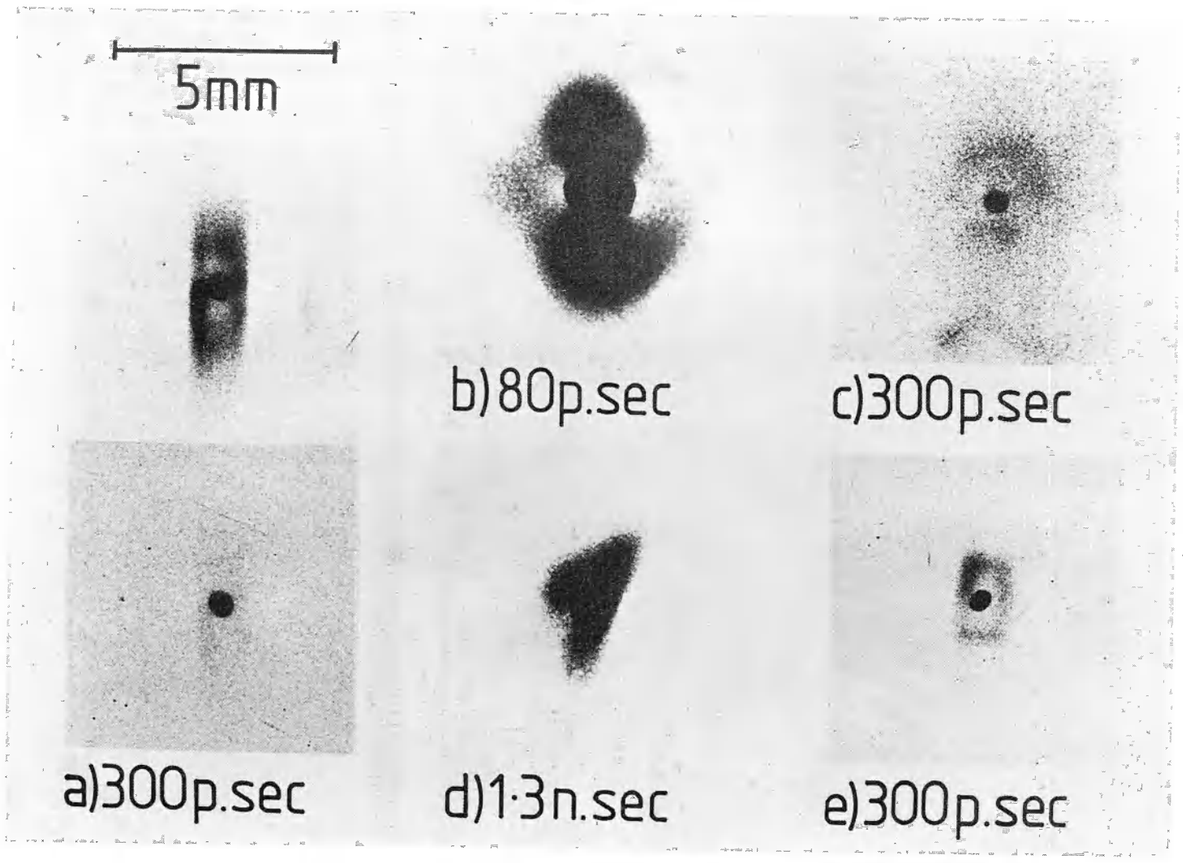

Fig. 2: (a) A pair of X-ray pinhole camera images of a 1 mm wide V strip irradiated with a 1.3 μm, 300 psec laser pulse focussed to 5 x 10^{15} W cm^{-2}. The upper and lower images were filtered by 12.5 μm Ti and 25 μm Sc respectively. Image (b) was for a 80 psec, 1.05 μm laser pulse at 1.8 x 10^{16} W cm^{-2} onto V, filtered by 12.5 μm Ti. Image (c) was for a 300 psec, 1.3 μm laser pulse focussed to 6 x 10^{15} W cm^2 onto Cu, and filtered by 11 μm Cu. Image (d) was as (b) except that the pulse was 1.3 nsec long focussed to 2 x 10^{15} W cm^{-2}. For images (b), (c) and (d) the targets were large area. For (e) the target was a 1 mm square of Cu and conditions were as in (c). In all cases the targets were thick to fast electrons with an area density > 6 mgm cm^{-2}.

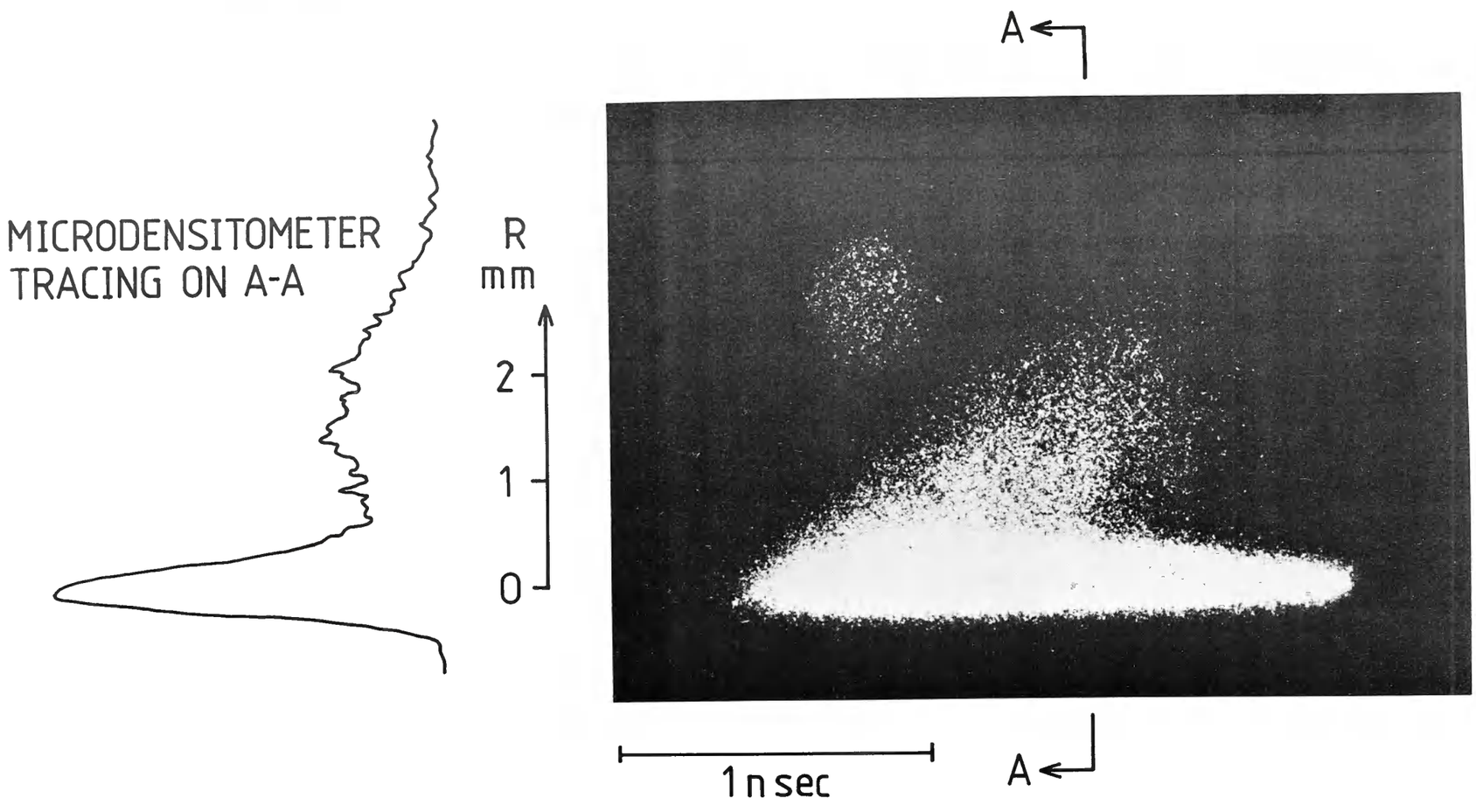

Fig. 3: An X-ray streak record of the emission from a V target through a 12.5 μm Ti K edge filter. The target, which was viewed obliquely, was irradiated at 2.6 x 10^{15} W cm^{-2} with a 1.3 nsec, 1.05 μm laser pulse. The bright emission at the bottom is the shadow of the μ mm imaging slit, which was displaced such that only one side of the spread emission at the bottom is the shadow of the 1 mm imaging slit, which was displaced such that only one side of the spread emission could be seen. The spot at the top left is an artefact.